



Article

Torque Ripple Reduction in Brushless Wound Rotor Vernier Machine Using Third-Harmonic Multi-Layer Winding

Muhammad Zulqarnain ¹, Sheikh Yasir Hammad ¹, Junaid Ikram ¹, Syed Sabir Hussain Bukhari ^{2,*} and Laiq Khan ¹

¹ Department of Electrical and Computer Engineering, COMSATS University Islamabad, Islamabad 45550, Pakistan; zulqur.sial@gmail.com (M.Z.); yasirhammad.02@gmail.com (S.Y.H.); junaidikram@comsats.edu.pk (J.I.); laiqkhan@comsats.edu.pk (L.K.)

² Electrical Engineering Unit, Tampere University, 33720 Tampere, Finland

* Correspondence: syed.bukhari@tuni.fi

Abstract: This article aims to realize the brushless operation of a wound rotor vernier machine (WRVM) by a third-harmonic field produced through stator auxiliary winding (X). In the conventional model, a third-harmonic current is generated by connecting a 4-pole armature and 12-pole excitation windings serially with a three-phase diode rectifier to develop a pulsating field in the airgap of a machine. However, in the proposed model, the ABC winding is supplied by a three-phase current source inverter, whereas the auxiliary winding (X) carries no current due to an open circuit. The fundamental MMF component developed in the machine airgap creates a four-pole stator field, while the third-harmonic MMF induces the harmonic current in the specialized rotor harmonic winding. The rotor on the other side contains the harmonic and the field windings connected through a full-bridge rectifier. The electromagnetic interaction of the stator and rotor fields generates torque. Due to the open-circuited winding pattern, the proposed machine results in a low torque ripple. A 2D model is designed using JMAG-Designer, and 2D field element analysis (FEA) is carried out to determine the output torque and machine's efficiency. A comparative performance analysis of both the conventional and proposed topologies is discussed graphically. The quantitative analysis of the proposed topology shows better performance as compared to the recently developed third-harmonic-based brushless WRVM topology in terms of output torque and torque ripples.



Citation: Zulqarnain, M.; Hammad, S.Y.; Ikram, J.; Bukhari, S.S.H.; Khan, L. Torque Ripple Reduction in Brushless Wound Rotor Vernier Machine Using Third-Harmonic Multi-Layer Winding. *World Electr. Veh. J.* **2024**, *15*, 163. <https://doi.org/10.3390/wevj15040163>

Academic Editors: Joeri Van Mierlo and Zhongze Wu

Received: 3 December 2023

Revised: 8 February 2024

Accepted: 10 April 2024

Published: 11 April 2024



Copyright: © 2024 by the authors. Licensee MDPI, Basel, Switzerland. This article is an open access article distributed under the terms and conditions of the Creative Commons Attribution (CC BY) license (<https://creativecommons.org/licenses/by/4.0/>).

1. Introduction

Electrical machines play a significant role in modern industries like textile mills, oil and gas, energy generation, and automotives. Various electric machines utilize permanent magnets (PMs) in the rotor structure. These machines are mostly used in traction applications to achieve high power density and high efficiency [1,2]. Permanent magnet synchronous machines (PMSMs) are being considerably developed because of the high energy density property of neodymium–iron–boron (NdFeB) magnets [3]. However, due to the high cost of rare earth magnets, researchers have developed multiple PM-less synchronous machine topologies. These topologies are either based on sub-harmonics or third-harmonics field excitation methods [4–10]. Traditional wound rotor synchronous machines (WRSMs) require brushes and slip rings to supply excitation current to the rotor field windings. However, due to the maintenance issues of mechanical contactors, i.e., slip rings and brushes, scientists have been paying attention to the brushless operation of WRSMs. To achieve the brushless operation of WRSMs, a phenomenon that develops an additional harmonic MMF component in the airgap of a machine has been realized by different researchers. This additional harmonic MMF component is developed using

different techniques mainly focused on stator winding configurations, input armature currents, and the stator slot's structure.

In [4], two inverters were used to inject different current magnitudes in two halves of stator armature windings. This tends to produce sub-harmonic and fundamental MMF components in the machine airgap. A harmonic winding and a field winding are the two windings that are placed on the rotor with a full-bridge rectifier connected between them. The generated sub-harmonic MMF is responsible for inducing the harmonic current in the harmonic winding that provides a rectified DC to the field winding. In this topology, two inverters were required for sub-harmonic MMF generation to achieve the brushless operation of a WRSM. To overcome this drawback, a brushless WRSM topology was implemented using a single inverter to generate a sub-harmonic MMF component [5]. In this scheme, the armature windings were distributed in a series-parallel combination (i.e., odd coils in series while the even coils were connected in parallel). The operation of this type of brushless machine was in such a way that the odd coils had the rated current, whereas the even coils were supplied with half of the rated current. This combination produced the sub-harmonic MMF component in the machine airgap along with the fundamental component. However, the difference in currents resulted in unbalanced radial forces and high torque ripple. To deal with these issues, another brushless scheme was proposed in [6]. The stator part in this scheme contains two windings, i.e., 4-pole armature windings and 2-pole excitation winding. Both windings contain the same number of turns and the machine is analyzed by supplying the same and different magnitudes of currents to both four-pole and two-pole windings to create fundamental and sub-harmonic MMF components in the airgap. The magnetic field lines were more uniformly distributed and improved efficiency was achieved in the case when both windings carry different magnitude of current. In [7], a novel scheme of brushless excitation for a four-pole, 24-slot WRVM was proposed. The employed schematic contained a three-phase four-pole armature and a single-phase two-pole excitation winding. Both windings were wound with the same number of turns and were coupled magnetically with each other. Here, a single-phase winding was designed with half the pole number in that of the main armature winding and a sub-harmonic MMF component was created to induce voltage into the harmonic winding of the rotor. In [8], a cost-effective brushless WRSM was realized with a single inverter which had a dual-armature winding configuration. This topology involved a four-pole main armature winding mutually coupled with a two-pole open-circuited winding. In [9], the brushless operation of WRSM was achieved by connecting thyristor switches in an anti-parallel direction with each phase. These switches were close to near zero-crossing of each phase, and the third-harmonic MMF was developed in the airgap of the machine. The continuous operation of thyristor switches causes higher torque ripples. Additionally, it increases the overall cost of the machine system due to the high number of switches. In addition, it involves control complications related to the operation of switches during its implementation. The other techniques used to achieve the third-harmonic excitation of WRSMs are through open-winding configuration and stator harmonic windings [10,11]. These topologies are based on a dual-converter configuration that makes the overall system bulky and costly. The use of high-order harmonics causes increased core losses which result in low efficiency.

To increase the torque capability for a WRSM, a brushless topology for a WRVM was introduced in [12]. A fundamental component and an additional sub-harmonic component were used for the excitation of the brushless rotor by using two inverters. In [13], a cost-effective brushless WRVM was proposed using a single inverter. The brushless configuration was achieved by incorporating XYZ windings in series with the armature winding, whose pole numbers were chosen in accordance with the excitation winding pole pairs. This model also achieved improved torque performance as compared to one proposed in [12]. Similar work was conducted by introducing a four-pole main armature and a two-pole excitation winding connected in series through an uncontrolled rectifier for sub-harmonic generation [14]. The topology was simple due to the single-phase winding, and

the excitation was improved, which led to higher torque as compared to the other vernier machines. Nevertheless, torque ripple was high, which was the main limitation of this topology. The torque performance of the brushless WRVM was also investigated by incorporating third-harmonic utilization [15]. A comparative analysis showed an improvement in average torque as compared to [12,13].

This paper presents an improved brushless operation of a WRVM. In the proposed brushless WRVM, an ABC winding is supplied by the three-phase current source inverter, whereas the auxiliary winding (X) carries no current due to being open-circuited but mutually connected with the main armature winding. The brushless operation is realized due to fundamental and third-harmonic MMF components developed in the machine airgap due to the specially designed three-phase four-pole winding, two-pole open winding, and slotting effect. The operating principle of the proposed topology is presented in Figure 1. Here, 2D-FEA was utilized for the performance analysis of the proposed WRVM under no load and load conditions. A performance comparative analysis of the proposed and recently developed brushless WRVM topology [14] was carried out in JMAG-Designer, which confirmed the improved torque characteristics and low torque ripple for the proposed brushless WRVM topology.

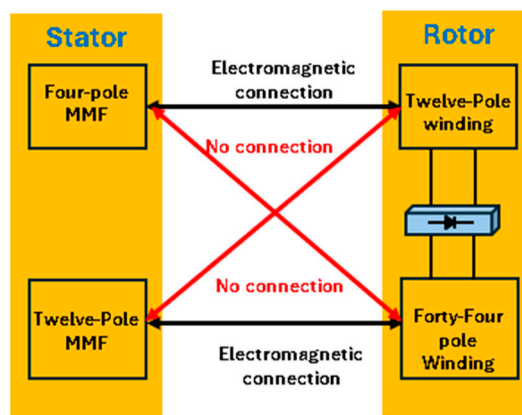


Figure 1. Operating principle of the proposed brushless WRVM.

2. Conventional Brushless WRVM Topology

Synchronous and vernier machines have different designs in terms of the number of poles on the stator and rotor. Equation (1) shows that to operate a vernier machine, the following relation must be satisfied:

$$P_r = N_s \pm P_s \quad (1)$$

where P_r represents rotor pole pairs, P_s is the representation of stator winding pole pairs, and N_s is the stator slot number.

In the conventional topology, a four-pole stator winding (ABC) is serially connected to a twelve-pole excitation winding (X) with a three-phase diode rectifier. The stator consists of 24 slots wounded with armature and excitation windings. The 2D design of the conventional model is shown in Figure 2. In order to create a third-harmonic component in the airgap, an armature winding is fed with a single inverter that supplies currents to both armature and series-connected excitation windings. A three-phase diode rectifier is connected between ABC and X, which delivers the pulsating DC to X when energized. In this way, fundamental and third-harmonic MMF components are generated due to the four- and twelve-pole stator winding configurations.

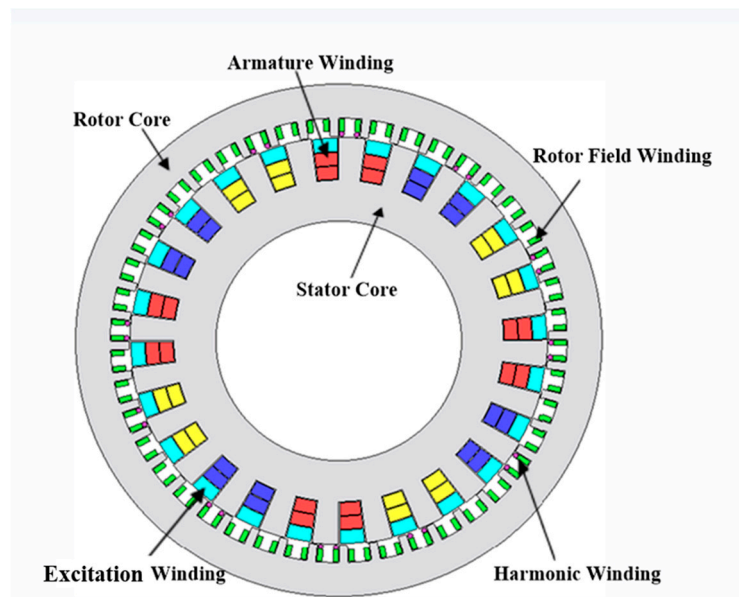


Figure 2. Two-dimensional design of the conventional brushless WRVM model.

The rotor part consists of harmonic and field windings which are connected through a full-bridge rectifier. A harmonic winding is used to obtain induced voltage to achieve the proposed brushless operation of the machine. The full-bridge rectifier is employed to provide DC to the field winding. Harmonic windings and excitation windings have the same number of poles. The rotor consists of 44 slots for a field winding and harmonic winding and is designed to have 44 poles for a field winding and 2 poles for a harmonic winding. This configuration is designed in a specific way to achieve the vernier mode of operation for the machine.

The schematic representation of the conventional brushless WRVM topology is presented in Figure 3. As shown in this figure, this topology consists of a main winding (ABC) and an excitation winding (X) connected with the full-bridge uncontrolled diode rectifier.

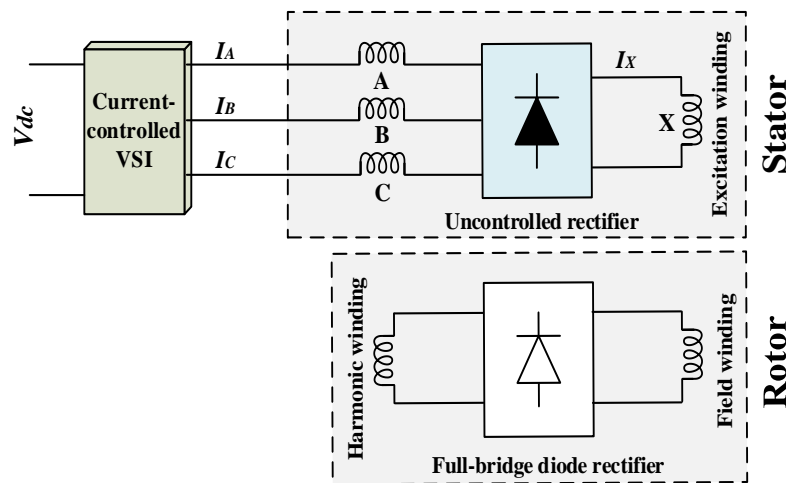


Figure 3. Conventional brushless WRVM topology.

3. Proposed Brushless WRVM Topology

For the proposed topology, a structural design similar to the conventional topology is adopted. However, in the case of the proposed topology, the auxiliary winding is open-circuited. The stator winding is designed with a multi-pole configuration, four-pole armature, and twelve-pole auxiliary winding. A twelve-pole auxiliary winding is

open-circuited, in which no current flows, but it is mutually connected with the main armature winding. In the proposed brushless WRVM, the auxiliary winding is designed to develop three times more poles than that of the main armature winding, which increases the machine's magnetic flux density. The structural design and 2D layout of the proposed brushless WRVM topology are shown in Figures 4 and 5, respectively. In comparison, the rotor of the machine consists of two windings, a twelve-pole harmonic winding and a forty-four-pole field winding. The harmonic winding has 12 poles to induce voltage in it due to the third-harmonic MMF component caused by the open winding configuration. The induced voltages are rectified to inject DC to the field winding and develop a 44-pole rotor magnetic field.

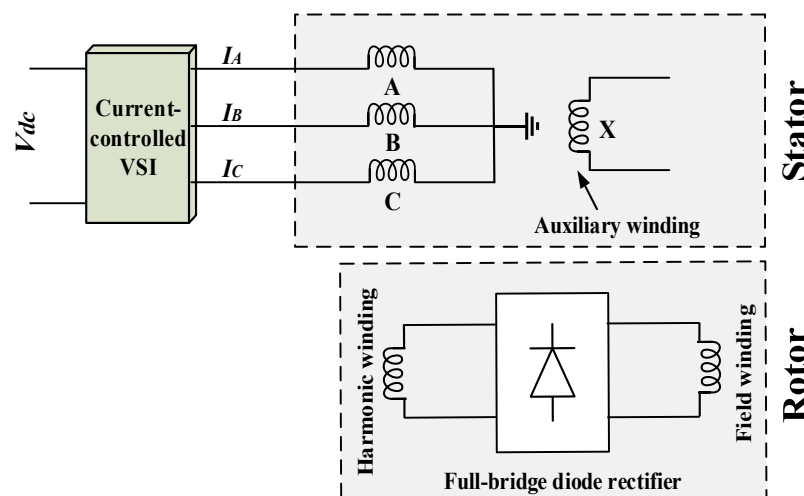


Figure 4. Proposed brushless WRVM topology.

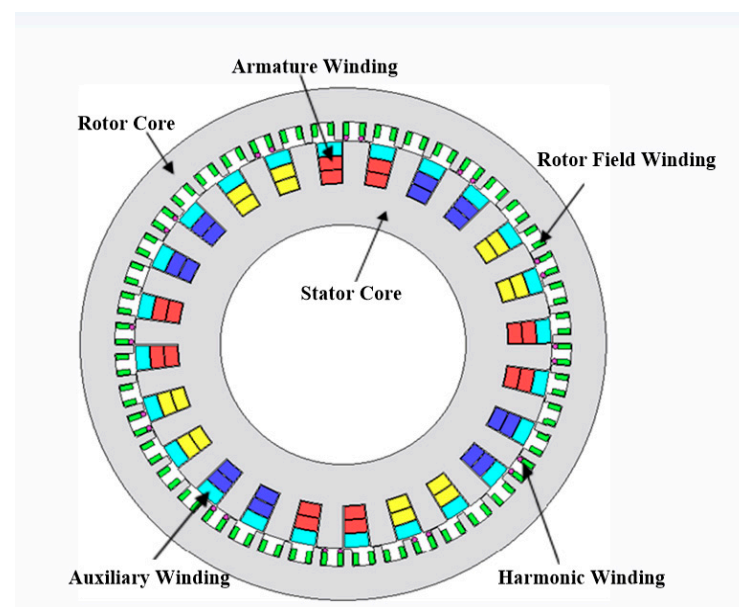


Figure 5. Two-dimensional design of the proposed brushless WRVM model.

Operating Principle

In the proposed brushless WRVM topology, the main armature winding (ABC) is supplied current from a single current-controlled voltage source inverter. On the other hand, the stator auxiliary winding (X) is placed near to the main armature winding which is open-circuited and carries no current. This arrangement results in an MMF in the airgap of the machine which consists of two components: (1) the fundamental component and

(2) the third-harmonic component. Figure 1 describes the simplified operating principle of a proposed third-harmonic-based brushless WRVM topology. The generated MMF components are electromagnetically linked with 12-pole rotor harmonic and 44-pole rotor field windings. The 12-pole third-harmonic MMF component induces a harmonic current in a dedicated 12-pole rotor harmonic winding, which is rectified to create a 4-pole rotor field. The interaction between the four-pole stator and rotor fields results in torque production.

As an auxiliary winding carries no current, the copper losses and torque ripple would be lower as compared to the conventional model. The induced voltage depends upon the following factors:

- Rotational speed of the machine;
- Flux in the machine;
- Basic construction (geometry) of the machine.

The full-bridge rectifier is employed in between the rotor harmonic and the field windings, which converts the induced voltage (AC) into direct current (DC). In this way, DC current field winding excitation is achieved without the use of brushes and slip rings. The three phase currents supplied to the main armature winding can be represented in the following equation:

$$\begin{aligned} i_a &= I_m \sin \omega_e t \\ i_b &= I_m \sin \left(\omega_e t - \frac{2\pi}{3} \right) \\ i_c &= I_m \sin \left(\omega_e t + \frac{2\pi}{3} \right) \end{aligned} \quad (2)$$

4. Design and 2D Finite Element Analysis of the Proposed Brushless WRVM Topology

The design of the proposed brushless WRVM consists of two parts: (1) stator design and (2) rotor design. The stator of the machine consists of an armature winding (ABC) and auxiliary winding (X). The design parameters of the proposed brushless wound rotor vernier machine are taken from [15]. The armature winding consists of four coils per phase, and these four coils are used to create four poles. The winding configuration of the proposed topology is calculated as follows:

$$\theta_e = \frac{P}{2} \theta_m = 4 \times 360/2 = 720^\circ \quad (3)$$

$$\theta_e/\text{slots} = 720/24 = 30^\circ$$

where P = number of poles in stator = 4; Number of slots = 24.

Figure 6 shows the winding distribution of the machine. In order to create the four-pole fundamental field for the proposed brushless WRVM, a distribution winding is used. The armature winding consists of four coils per phase, and these four coils are used to create four poles in the stator.

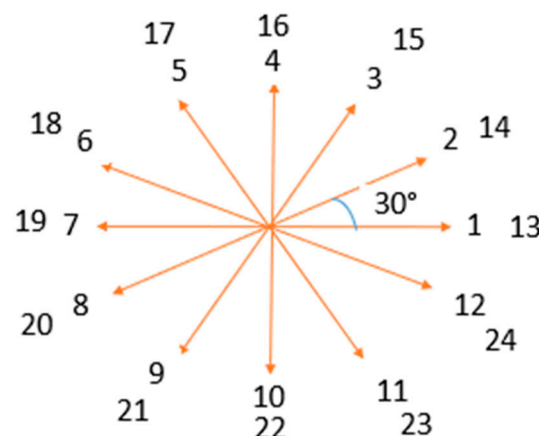


Figure 6. Slots arrangement for stator pole.

Finite element analysis (FEA) is used to solve the partial differential or integral equations which otherwise cannot be solved accurately. For the performance analysis of the conventional and proposed brushless WRVM topologies, FEA analysis is carried out under no-load and load conditions. The design parameters of the conventional and proposed machine models are presented in Table 1.

Table 1. Design parameters of the conventional and proposed machine models.

Parameters	Units	Conventional Model	Proposed Model
Stator poles	-	4	4
Stator slots	-	24	24
Stator inner diameter	mm	140	140
Stator outer diameter	mm	238	238
Stator winding turns	-	90	90
Rotor field winding turns	-	36	36
Rotor harmonic winding turns	-	6	6
Stator excitation winding turns	-	90	24
Rotor field poles	-	44	44
Rotor slots	-	44	44
Rotor inner diameter	mm	239	239
Rotor outer diameter	mm	300	300
Stator XYZ winding turns	-	90	90
Stator XYZ poles	-	2	2
Slots for XYZ winding	-	6	6
Operating speed	rpm	300	300
Airgap	mm	0.5	0.5

4.1. No-Load Case Analysis

For the no-load analysis of the conventional and proposed brushless WRVM topologies, a DC current of 10 A DC is supplied to the field winding of the machines. Figures 7 and 8 show the back-EMF of the conventional and proposed brushless WRVM topologies. The Fast Fourier Transform (FFT) of no-load back-EMF for the proposed model is presented in Figure 9, showing the harmonic contents of the back-EMF produced for the proposed topology under the no-load condition. It can be observed that, other than the fundamental component, the third-harmonic component is most dominant, which induces EMF in the specialized rotor harmonic winding. The airgap flux density is shown in Figure 10. The graphic representation shows that the rotor field winding has 22-pole pairs. On the other hand, the stator windings have two-pole pairs. Because “magnetic gearing” is used in vernier machines, the machine itself acts as a vernier and generates torque. The root mean square (RMS) value of the back-EMF of the conventional and proposed models is 209.01 V_{RMS} and 216 V_{RMS}, respectively. These figures show that the proposed model produces 3.34% higher back-EMF as compared to the conventional model.

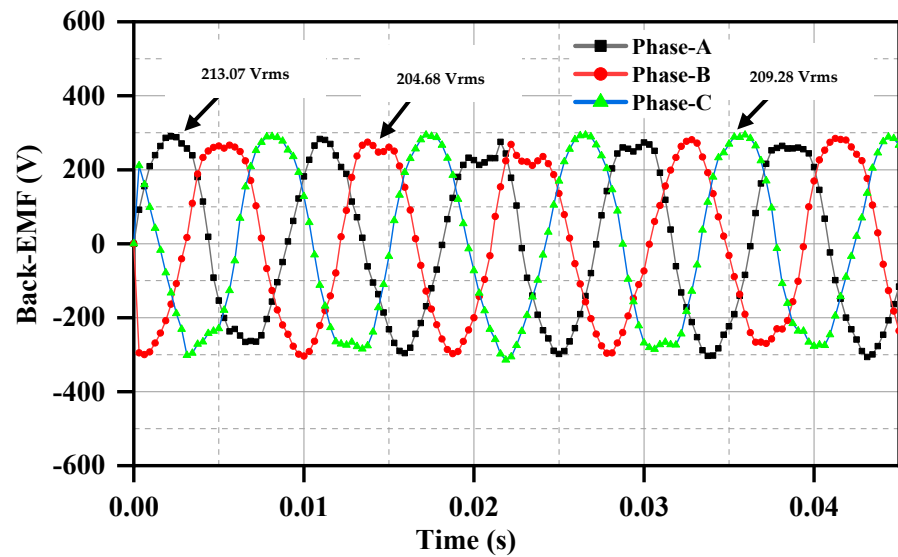


Figure 7. No-load back-EMF of the conventional topology.

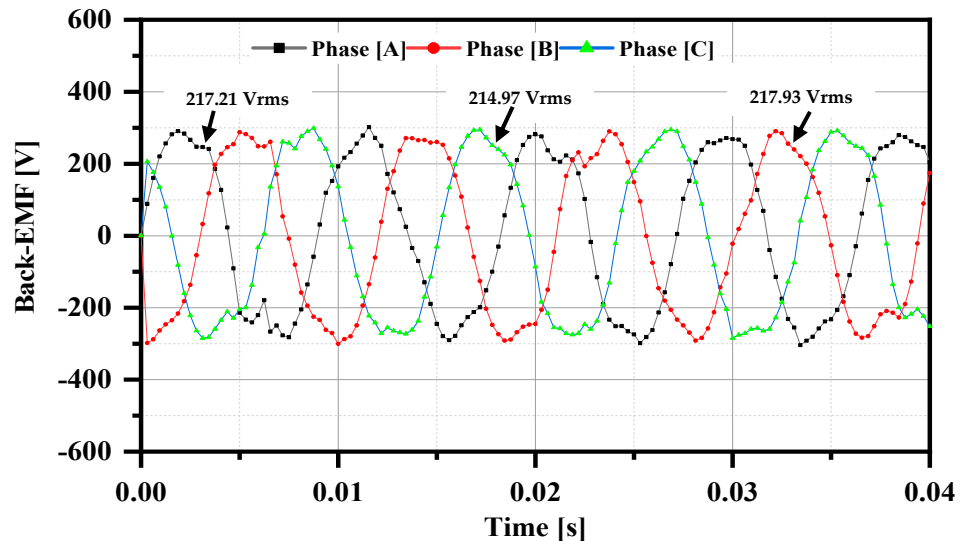


Figure 8. No-load back-EMF of the proposed topology.

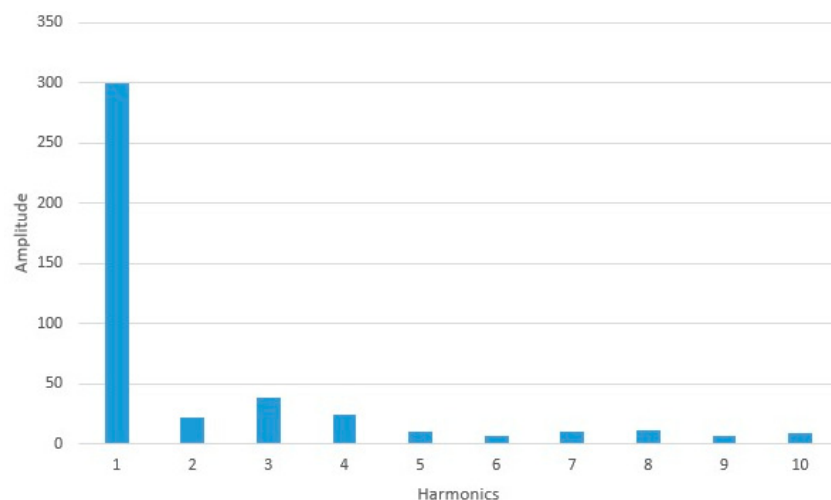


Figure 9. FFT of back-EMF under the no-load condition for the proposed topology.

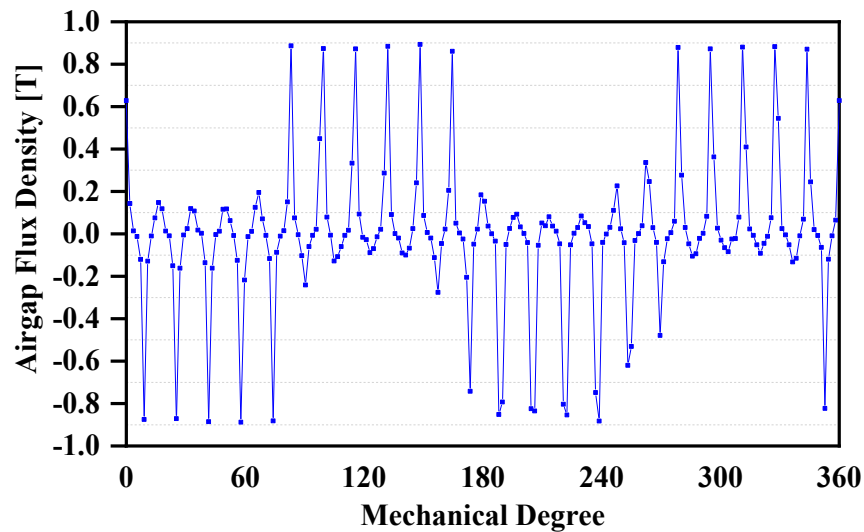


Figure 10. Airgap flux density of the proposed model.

4.2. Load Case Analysis

The shaft of the conventional and proposed machine brushless WRVM models is operated at a speed of 300 rpm in order to analyze their behavior under load conditions. The conventional brushless topology contains three-phase windings (ABC) and excitation windings (X) connected in series through a three-phase rectifier. The armature winding is supplied with a current of 2.12 A (rms) which is shown in Figure 11. For the better comparative performance analysis, the proposed topology is supplied with similar currents as in the case of the conventional topology.

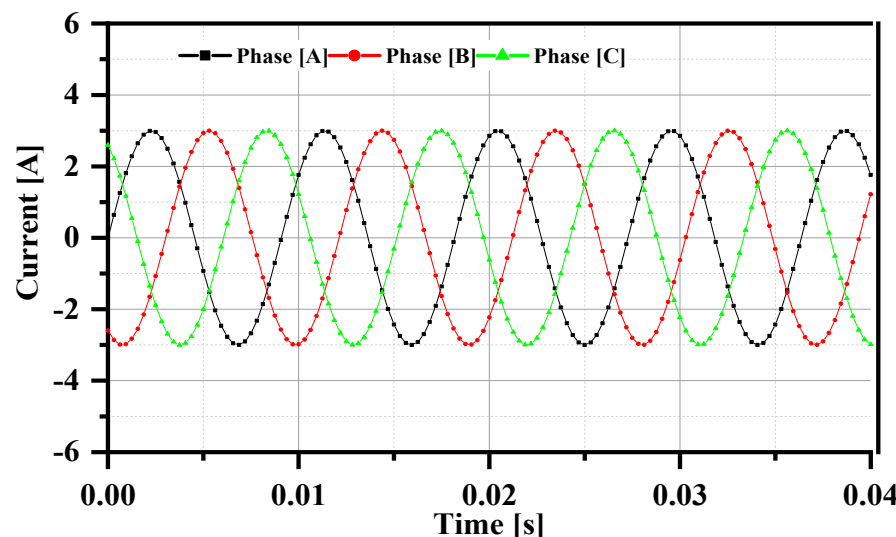


Figure 11. Armature currents for the conventional and proposed models.

The stator auxiliary winding of a the proposed brushless WRVM is open-circuited, by which no current flows through the excitation winding, providing a low reluctance path to the flux lines by which its magnetic flux density under load conditions increases. Due to this, a sufficient voltage is induced in the specially designed rotor harmonic winding. A full-bridge rectifier then rectifies this induced voltage. The airgap flux density of a proposed model under load conditions is shown in Figure 12, whereas the voltage induced in the rotor harmonic winding is shown in Figure 13. The rectified DC is transferred to the rotor field winding to generate a 44-pole field. The rectified field voltages are shown in Figure 14. In the proposed model, the field current increases due to the increase in the number of

poles in the machine and the third-harmonic MMF component in the machine airgap. Field current graphs of the conventional and proposed models are shown in Figure 15a,b, respectively.

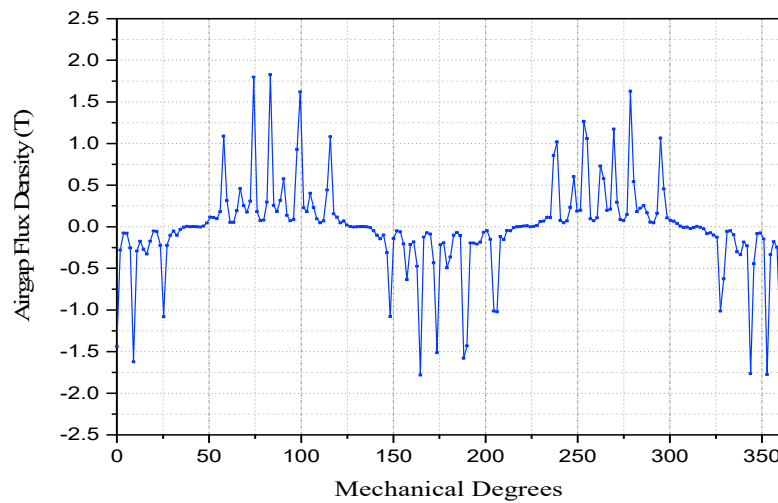


Figure 12. Magnetic flux density under load conditions of the proposed model.

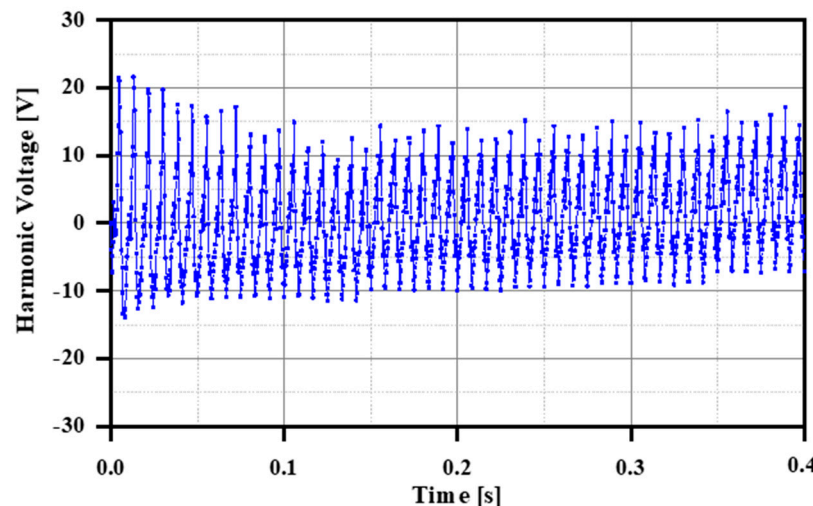


Figure 13. Induced voltages in the harmonic winding of the proposed model.

The load torque developed in the conventional and proposed models is about 41.01 Nm and 39.74 Nm, respectively. Torque characteristics are shown in Figure 16a,b for the conventional and proposed models. As an auxiliary winding has zero current, the impact is negligible. Due to this, the load torque developed by the proposed model is 3.12% lower compared to the conventional model; however, its torque ripple is 24.24% lower than that of the conventional model.

The aim of this research is to design a brushless WRVM to reduce the torque ripple as compared to the conventional model. For this, the auxiliary winding in the proposed brushless WRVM carries no current due to its open-winding configuration. The winding is designed to create 12-pole magnetic flux that increases its field intensity. The obtained results show that the torque ripple is reduced significantly as compared to the conventional brushless WRVM. For further analysis, the proposed brushless WRVM is investigated by supplying separate DC and AC currents to the 12-pole auxiliary winding.

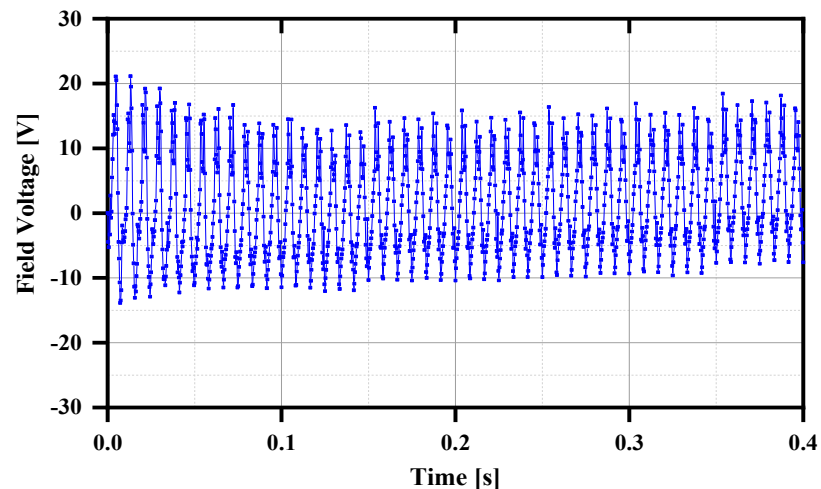


Figure 14. Field winding voltages of the proposed model.

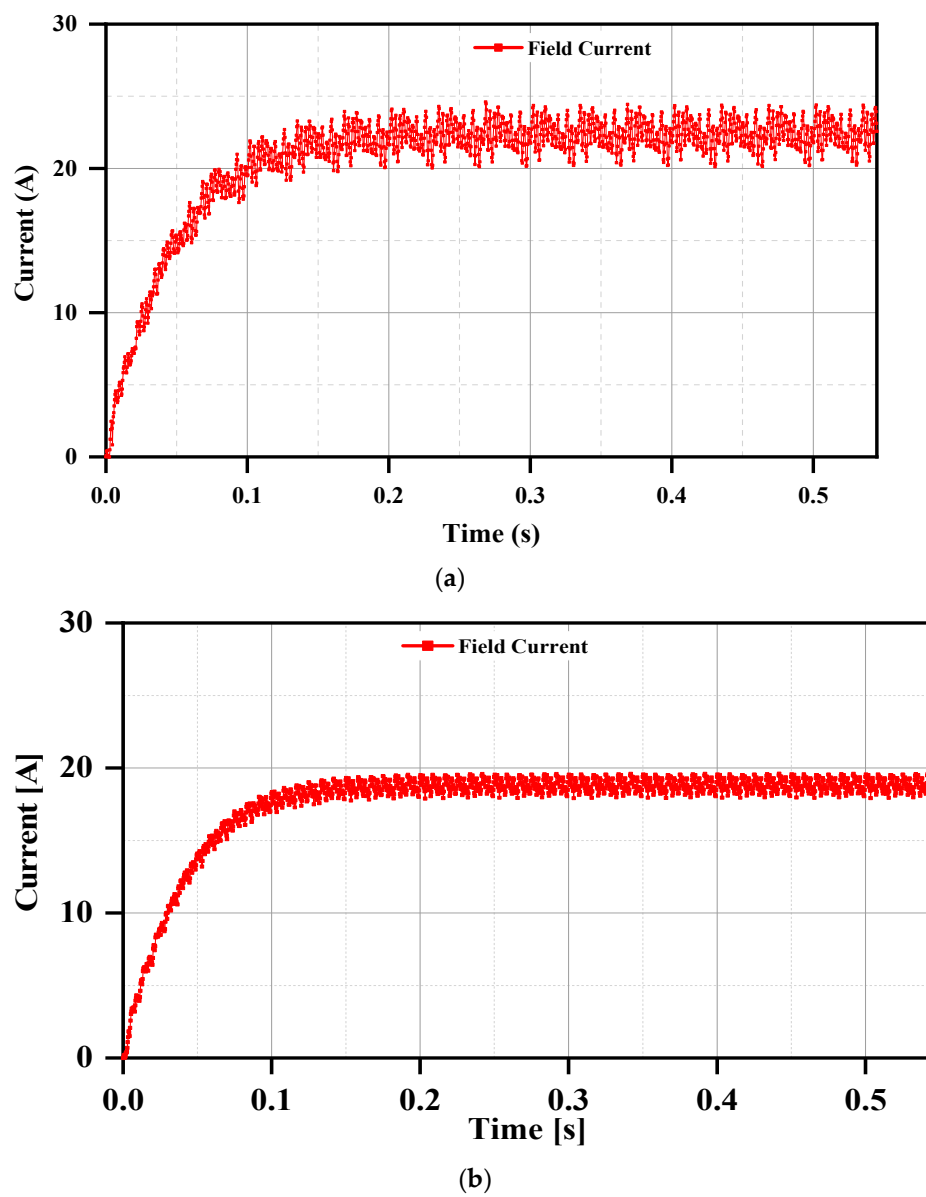


Figure 15. Field current of (a) conventional model and (b) proposed model.

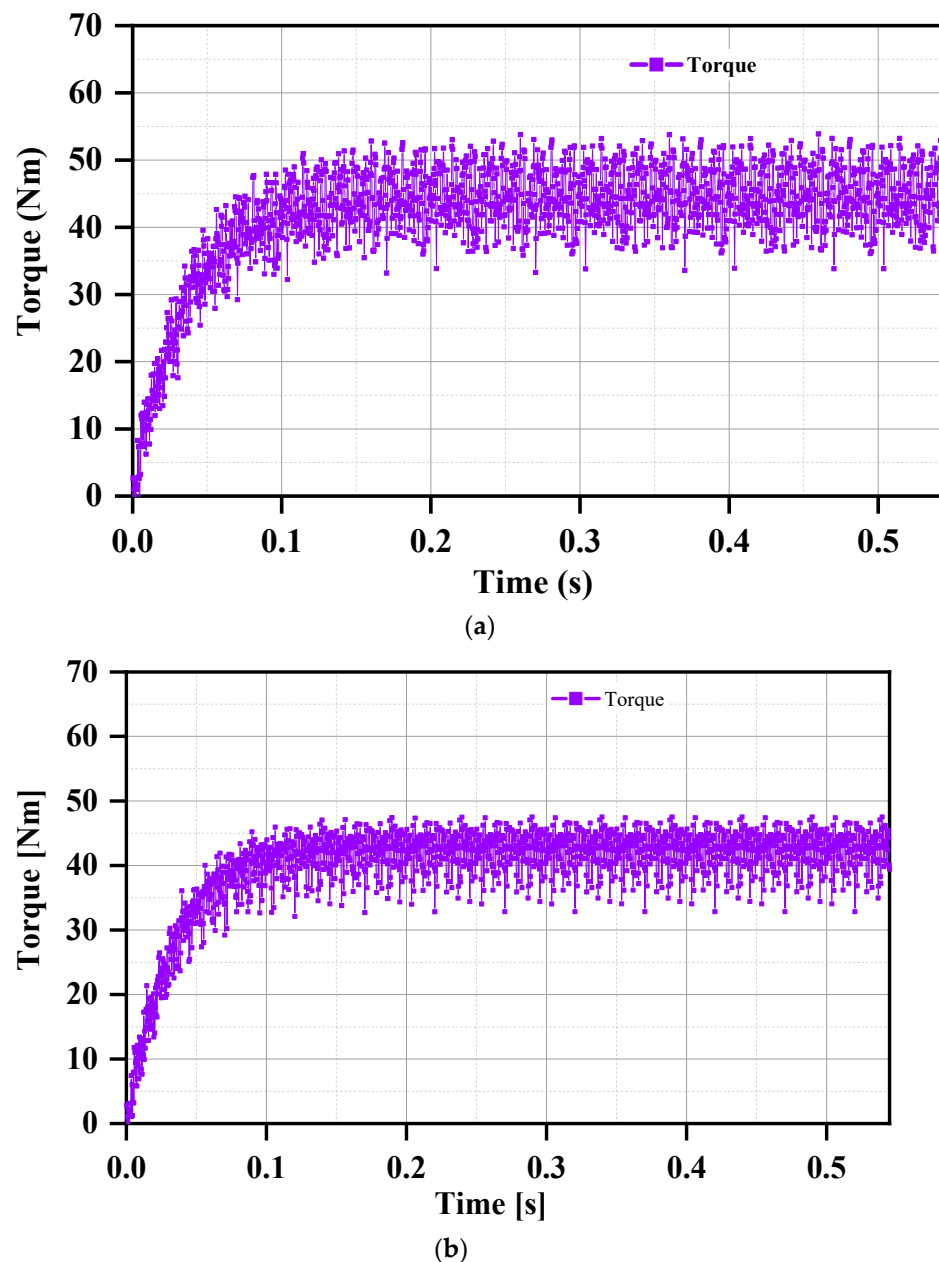


Figure 16. Torque of (a) conventional model and (b) proposed model.

The simulation results for the proposed brushless WRVM machine are classified into three cases: (1) case I: open-winding configuration for an auxiliary winding, (2) case II: supplying a 12-pole winding with a DC current, and (3) supplying a 12-pole winding with an AC current. The same (rms) current of 2.12 A is supplied to the armature winding, while the stator auxiliary winding carries 5.32 A (rms), which is the same current that flows through the excitation winding of the conventional model. Figure 17 shows the comparative field current results of case II and III. These results show that the field current developed by supplying the AC source is 25.51 A.

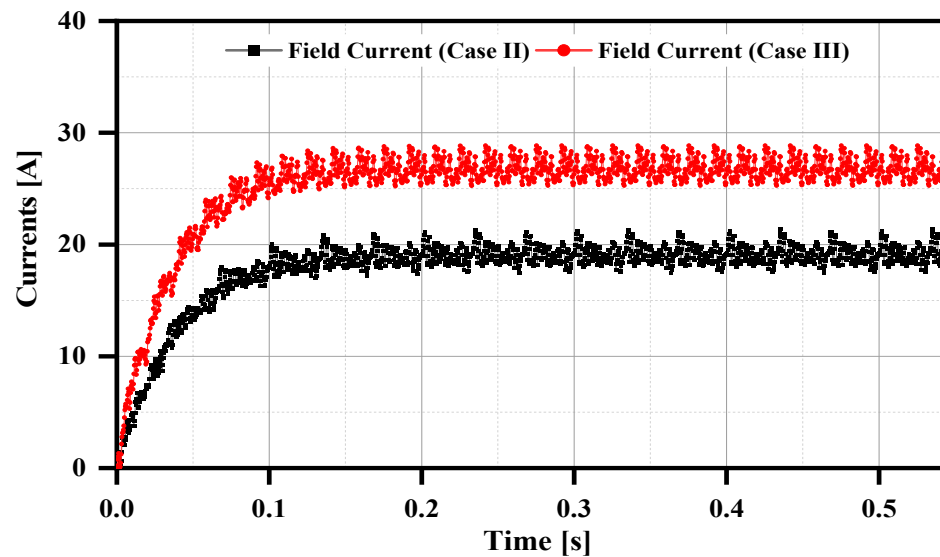


Figure 17. Comparative results of field currents.

The field currents of the proposed topology in case II are almost the same as those of the conventional topology (shown in Figure 15), which is around 17.85 A. This means that the load torque of the proposed topology will be higher in case III as compared to case I, case II, and conventional topology. Figure 18 shows the comparative results of the load torque. The load torque developed in case II is around 39.23 Nm.

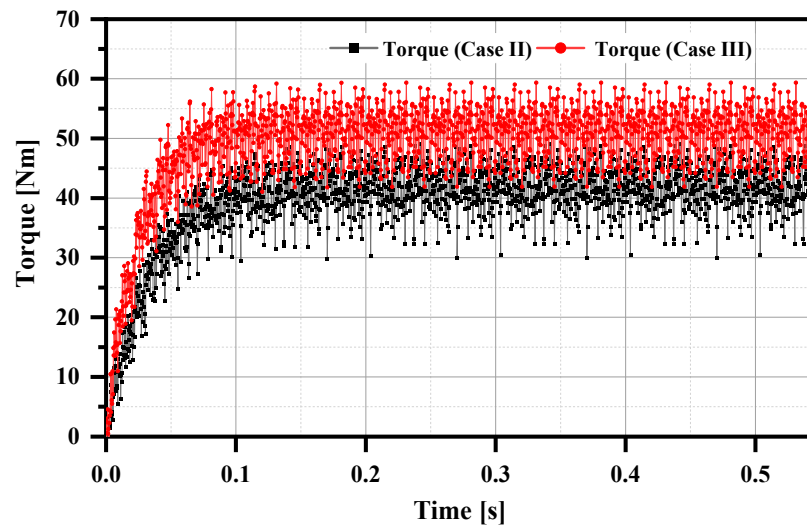


Figure 18. Comparative result of load torque.

The load torque in case II is slightly decreased even from Case I. The reduction in load torque may be due to higher magnetic saturation, which could be avoided through the optimization process in the future. The average load torque developed in case III is 48.8 Nm, which is 22.86% and 14.11% higher than case II and the conventional model. The torque ripple of the proposed topology in case II and case III is 36.52% and 35.68%, respectively. The reduction in torque ripple in case III is 5.15% when compared to case I and 27.18% from the conventional model. Hence, these results show that the proposed model is advantageous in reducing torque ripple as compared to the conventional model.

The harmonic currents of case II and III are shown in Figure 19a,b. The graphs illustrate that the harmonic winding in case III induces higher harmonic currents with an rms value of 19.35 A due to changes in electromagnetic induction. This helps to induce a higher

rectified field current in the field windings in Figure 17. Due to its higher harmonic current, the copper loss in case III is higher as compared to case II.

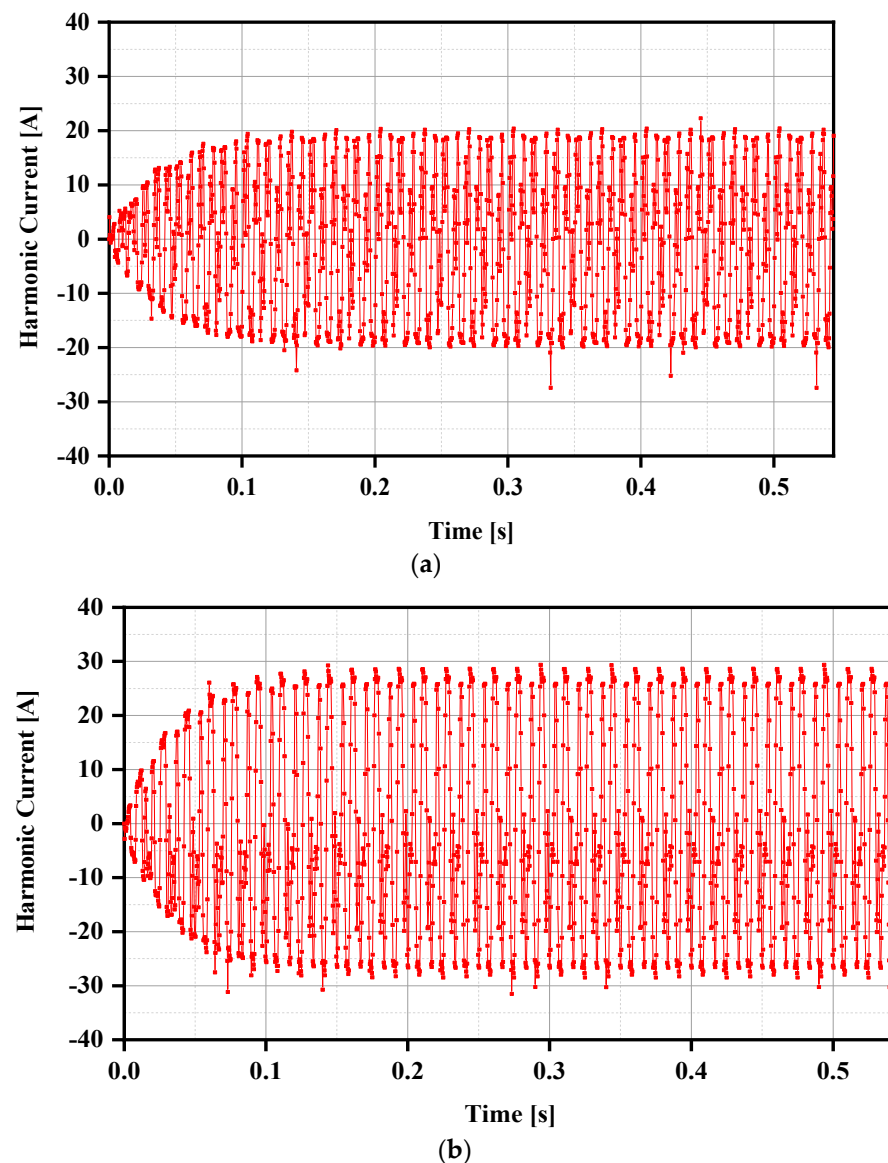


Figure 19. Harmonic currents in (a) case II and (b) case III.

Figure 20 shows the comparison of losses of the conventional model and case I, II, and III of the proposed models. In case I, the open-circuited configuration mutually links the auxiliary winding with the main armature winding, increasing magnetic flux by three times due to a greater number of poles. Due to higher magnetic flux as shown in Figure 12, there is an increase in energy losses, by which the hysteresis losses increase and, hence, the iron losses are higher, while the eddy current losses are ignorable due to no current.

On the other hand, in case II, the core losses are higher as compared to case III, and the efficiency of case II is decreased by 5.43%.

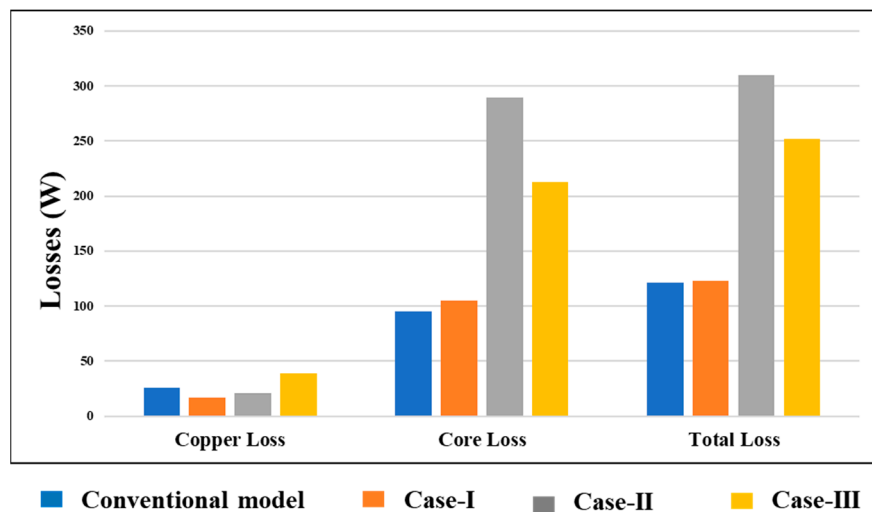


Figure 20. Losses of conventional and proposed models.

5. Comparative Analysis

In this analysis, the conventional and proposed models (case I, II, and III) are compared to determine the machine's performance. Table 2 shows that torque magnitude is significantly increased with reduced torque ripples in the proposed models.

Table 2. Comparative analysis.

Parameters	Unit	Conventional Topology	Proposed Topology (Case I)	Proposed Topology (Case II)	Proposed Topology (Case III)
Armature currents	[A]	ABC = 2.12 (rms) X carries 5.32 (rms)	ABC = 2.12 (rms) X carries no current	5.32 (rms)	5.32 (rms)
Torque	[Nm]	41.91	39.74	39.23	48.8
Torque ripple	%	49	36.90	36.52	35.68
Field current	[A]	20.55	17.53	17.85	25.51
Copper losses	[W]	25.98	17.17	21.07	38.94
Core losses	[W]	95.02	105.09	289.06	212.77
Total losses	[W]	121	122.8	310.13	251.71
Output power	[W]	1661.84	1588.2	1576	1863.34
Efficiency	η	93.21	93	83.55	88.09

6. Conclusions

This paper proposes a third-harmonic-based brushless WRVM in which a single inverter and multi-layer winding configuration is used. The proposed topology uses armature and auxiliary windings that employ 24-stator slots generating fundamental and third-harmonic MMF. The proposed topology uses a less-rectifying stage system which makes the system very simple as compared to the conventional model. The FEA results validate the proposed topology that shows a significant decrease in torque ripple of about 24.24%, while there is a slight decrease in load torque.

In comparison with the conventional model, the auxiliary winding in the proposed model is fed with an AC/DC source to verify the results more precisely. The main purpose of supplying the same (rms) value with two different sources was for a reasonable comparison between the conventional and proposed topologies. By supplying the AC source, the electromagnetic results show that the load torque is 22.86% higher than the DC source and open-circuited pattern. When comparing case III with case II, the torque ripple is slightly reduced to 5.15%.

Finally, results were concluded by analyzing the comparative analysis, which shows better performance on the basis of load torque and torque ripple. Total losses are increased, due to which, the efficiencies of the machine in case II and III are slightly reduced because of the higher current supplied to the auxiliary winding as compared to case I. In contrast, the proposed brushless topology of the WRVM is simple, as it is a single rectifying system used in the rotor as compared to the conventional topology, which is a two-stage rectifying system used in both the stator and rotor.

Author Contributions: Conceptualization, J.I. and S.S.H.B.; methodology, M.Z. and S.Y.H.; software, S.S.H.B.; validation, M.Z. and S.Y.H.; formal analysis, M.Z. and S.Y.H.; writing—review and editing, L.K. All authors have read and agreed to the published version of the manuscript.

Funding: This research received no external funding.

Data Availability Statement: The original contributions presented in the study are included in the article, further inquiries can be directed to the corresponding author.

Conflicts of Interest: The authors declare no conflicts of interest.

References

1. Du, Z.S.; Lipo, T.A. Efficient Utilization of Rare Earth Permanent-Magnet Materials and Torque Ripple Reduction in Interior Permanent-Magnet Machines. *IEEE Trans. Ind. Appl.* **2017**, *53*, 3485–3495. [[CrossRef](#)]
2. Barcaro, M.; Bianchi, N. Interior PM Machines Using Ferrite to Replace Rare-Earth Surface PM Machines. *IEEE Trans. Ind. Appl.* **2013**, *50*, 979–985. [[CrossRef](#)]
3. Bash, M.; Pekarek, S.; Sudhoff, S.; Whitmore, J.; Frantzen, M. A comparison of permanent magnet and wound rotor synchronous machines for portable power generation. In Proceedings of the IEEE 2010 Power and Energy Conference at Illinois (PECI), Urbana, IL, USA, 12–13 February 2010.
4. Ali, Q.; Lipo, T.A.; Kwon, B.-I. Design and Analysis of a Novel Brushless Wound Rotor Synchronous Machine. *IEEE Trans. Magn.* **2015**, *51*, 8109804. [[CrossRef](#)]
5. Ayub, M.; Hussain, A.; Jawad, G.; Kwon, B.-I. Brushless Operation of a Wound-Field Synchronous Machine Using a Novel Winding Scheme. *IEEE Trans. Magn.* **2019**, *55*, 8201104. [[CrossRef](#)]
6. Humza, M.; Yazdan, T.; Ali, Q.; Cho, H.W. Brushless Operation of Wound-Rotor Synchronous Machine Based on Sub-Harmonic Excitation Technique Using Multi-Pole Stator Windings. *Mathematics* **2023**, *11*, 1117. [[CrossRef](#)]
7. Humza, M.; Yazdan, T.; Siddiqi, M.R.; Wook-Cho, H. Brushless Wound Rotor Vernier Motor Using Single-Phase Additional Winding on Stator for Variable Speed Applications. *IEEE Access* **2023**, *11*, 86262–86270. [[CrossRef](#)]
8. Bukhari, S.S.H.; Shah, M.A.; Rodas, J.; Bajaj, M.; Ro, J.-S. Novel sub-harmonic-based self-excited brushless wound rotor synchronous machine. *IEEE Can. J. Electr. Comput. Eng.* **2022**, *45*, 365–374. [[CrossRef](#)]
9. Jawad, G.; Ali, Q.; Lipo, T.A.; Kwon, B.-I. Novel Brushless Wound Rotor Synchronous Machine with Zero Sequence Third Harmonic Field Excitation. *IEEE Trans. Magn.* **2016**, *52*, 1. [[CrossRef](#)]
10. An, Q.; Gao, X.; Yao, F.; Sun, L.; Lipo, T. The structure optimization of novel harmonic current excited brushless synchronous machines based on open winding pattern. In Proceedings of the 2014 IEEE Energy Conversion Congress and Exposition (ECCE), Pittsburgh, PA, USA, 15–18 September 2014; pp. 1754–1761.
11. Sirewal, G.J.; Ayub, M.; Atiq, S.; Kwon, B.I. Analysis of a brushless wound rotor synchronous machine employing a stator harmonic winding. *IEEE Access* **2020**, *8*, 151392–151402. [[CrossRef](#)]
12. Ali, Q.; Hussain, A.; Baloch, N.; Kwon, B.I. Design and Optimization of a Brushless Wound-Rotor Vernier Machine. *Energies* **2018**, *11*, 317. [[CrossRef](#)]
13. Tariq, S.; Ikram, J.; Bukhari, S.S.H.; Ali, Q.; Hussain, A.; Ro, J.-S. Design and Analysis of Single Inverter-Fed Brushless Wound Rotor Vernier Machine. *IEEE Access* **2022**, *10*, 101609–101621. [[CrossRef](#)]
14. Bukhari, S.S.H.; Ikram, J.; Wang, F.; Yu, X.; Imtiaz, J.; Rodas, J.; Ro, J.-S. Novel Self-Excited Brush-Less Wound Field Vernier Machine Topology. *IEEE Access* **2022**, *10*, 97868–97878. [[CrossRef](#)]
15. Hammad, S.Y.; Ikram, J.; Badar, R.; Bukhari, S.S.H.; Khan, L.; Ro, J.-S. Performance Analysis of Brushless Wound Rotor Vernier Machine by Utilizing Third Harmonic Field Excitation. *IEEE Access* **2023**, *11*, 65480–65490. [[CrossRef](#)]

Disclaimer/Publisher’s Note: The statements, opinions and data contained in all publications are solely those of the individual author(s) and contributor(s) and not of MDPI and/or the editor(s). MDPI and/or the editor(s) disclaim responsibility for any injury to people or property resulting from any ideas, methods, instructions or products referred to in the content.